THE ASTROPHYSICAL JOURNAL, 266:41–57, 1983 March 1

THE KINEMATIC PROPERTIES OF FAINT ELLIPTICAL GALAXIES

ROGER L. DAVIES,[1,3] GEORGE EFSTATHIOU,[1] S. MICHAEL FALL,[1,2] GARTH ILLINGWORTH,[3] AND PAUL L. SCHECHTER[3]

Received 1982 March 23; accepted 1982 August 20

ABSTRACT

We have measured the rotation curves and velocity dispersion profiles for 11 faint elliptical galaxies ($M_B \geq -20.8$ taking $H_0 = 50$ km s^{-1} Mpc^{-1}). Central velocity dispersions have been obtained for an additional six faint ellipticals. We find that faint ellipticals rotate more rapidly than bright ellipticals and almost as rapidly as predicted by models with oblate figures and isotropic distributions of residual velocities. In the present sample, there is no significant difference between the rotational properties of the bulges of disk galaxies and ellipticals with similar absolute magnitudes when differences in their ellipticities are taken into account. We also investigate the relation between central velocity dispersion and luminosity and find some indication that it may be steeper at low luminosities. Our results show that it may be possible to satisfy the empirical correlation between rotation and luminosity if ellipticals formed in a clustering hierarchy, but the slow rotation of bright ellipticals is difficult to reconcile with their high densities. The decrease of rotation with luminosity is in the sense expected if ellipticals formed by merging or by fragmentation in pancakes.

Subject headings: galaxies: internal motions — galaxies: formation — galaxies: structure

I. INTRODUCTION

In the last 5 years, the kinematic properties of several dozen elliptical galaxies have been inferred from the displacement and broadening of the absorption lines in their spectra (Illingworth 1981, and references therein). The resulting profiles of rotation velocity and velocity dispersion are conveniently summarized in terms of the ratio of V_m, the maximum rotation velocity along the major axis, to σ_0, the velocity dispersion at the center of the galaxy. In most cases, V_m/σ_0 is found to be substantially lower than the value required for an oblate system of the observed shape with an isotropic distribution of residual velocities. From the scatter diagram of V_m/σ_0 against ellipticity, one may conclude that these galaxies are deformed by anisotropic stresses rather than by rotation (Binney 1981, and references therein).

Nearly all the ellipticals studied to date are bright, with absolute magnitudes $M_B \lesssim -20.5$, and the question naturally arises as to whether rotation is also of little significance in faint ellipticals. Any dependence of V_m/σ_0 on M_B should help to discriminate among various theories for the origin of angular momentum and the formation of elliptical galaxies, such as those involving dissipative collapse (Larson 1975) or merging (Toomre 1977). We have therefore measured the rotation curves and velocity dispersion profiles of 11 faint ellipticals, with the intention of comparing them with their brighter counterparts.

A second motivation for this study came from observations of the bulges of disk galaxies. Ellipticals and bulges have similar surface brightness profiles (de Vaucouleurs 1959) and, at a given luminosity, they have similar broad-band colors (Sandage and Visvanathan 1978), metallic line strengths (Faber 1977), and velocity dispersions (Whitmore, Kirshner, and Schechter 1979). These relations suggest that ellipticals and bulges may be fundamentally the same kind of object and share a common origin. Recent measurements of the rotation velocities and velocity dispersions in the bulges of disk galaxies show that these oblate systems have values of V_m/σ_0 that are comparable to those required for isotropic velocity distributions (Illingworth and Schechter 1982; Kormendy and Illingworth 1982; Kormendy 1982). Most of these bulges have absolute magnitudes in the range $-18.5 \gtrsim M_B \gtrsim -20.5$ and are therefore fainter than most of the previously studied ellipticals. The observations reported here allow for a direct comparison between the kinematic properties of these systems.

The plan for the remainder of the paper is as follows. In § II we report the details of our observations, our reduction procedures, and the resulting rotation curves and dispersion profiles. In § III we compare our results with those obtained for brighter ellipticals and the bulges of disk galaxies. In § IV we discuss briefly the theoretical implications of these observations, and in § V we summarize our main conclusions.

II. DATA

a) Selection of Galaxies

There are few intrinsically faint ellipticals that are apparently bright enough to be observed with the required resolution (50–70 km s^{-1}). In the Virgo Cluster for example, a galaxy with $M_B = -18$ has $B_T \approx 13$–14,

[1] Institute of Astronomy, University of Cambridge.
[2] Institute for Advanced Study, Princeton, New Jersey.
[3] Kitt Peak National Observatory, operated by the Association of Universities for Research in Astronomy, Inc., under contract with the National Science Foundation.

which is faint enough to make measurement difficult. Our initial selection was based upon the classifications, B_T magnitudes, and velocities given in the *Second Reference Catalogue of Bright Galaxies* (de Vaucouleurs, de Vaucouleurs, and Corwin 1976, hereafter RC2). This sample was supplemented by a few galaxies in the *Uppsala General Catalogue of Galaxies* (Nilson 1973, hereafter UGC). The classifications were checked against the UGC, the ESO/Uppsala Catalogue (e.g., Lauberts *et al.* 1981 and references therein), and *A Revised Shapley-Ames Catalog of Bright Galaxies* (Sandage and Tammann 1981, hereafter RSA). In only two cases was there any ambiguity between E and S0 classifications. As in earlier kinematic studies, our sample is slightly biased toward flattened ellipticals. The implications of these points are discussed in detail in § III.

b) *Observations*

The Cassegrain spectrographs at the 3.9 m Anglo-Australian Telescope (AAT) and the Kitt Peak National Observatory (KPNO) 4 m telescope were used to acquire data for this project. The detector systems used were the image photon counting system (IPCS) and the high gain video spectrometer (HGVS) respectively. Table 1 summarizes the details of the instrumental configurations. The observational procedures that we adopted for this project are similar to those described in detail by Davies (1981) for the AAT system and by Kormendy and Illingworth (1982) for the KPNO system. Galaxy exposures were interspersed with exposures of the comparison lamp to monitor the geometric stability. Typical galaxy exposure times were 1200 s at the AAT and 1700 s at KPNO. Appropriate flat-field frames were also taken. The small size of the galaxies allowed us to derive satisfactory sky spectra from the edges of each data frame.

Eleven galaxies were observed for sufficient time to allow rotation curves and velocity dispersion profiles to be determined. Lower signal-to-noise spectra of seven galaxies were obtained in a moonlit half-night at the AAT, and only central velocity dispersions could be measured from them. The objects observed, their Hubble types, the position angle of the spectrograph slit (measured N through E), and the total integration times are given in Table 2A. During twilight, several G and K giant stars were observed for use as templates in the determination of velocities and velocity dispersions by the cross-correlation and Fourier quotient techniques. The details of these observations are given in Table 2B.

TABLE 1

OBSERVED CONFIGURATIONS

Parameter	AAT	KPNO
Detector	IPCS	HGVS
Pixel size	2.″4	1.″4
Frame format	52 × 2044	128 × 512
Spectrograph	RGO	RC
Slit width	2.″0	2.″5
Slit length	2.′0	2.′9
Dispersion	33 Å mm^{-1}	25/50[a] Å mm^{-1}
Instrumental resolution	50 km s^{-1}	70/150[a] km s^{-1}
Wavelength range	4650–5672 Å	4140–4490 Å
Spatial resolution	2.″4	2.″5–3.″5

[a] Lower resolution used only for NGC 2778.

c) *Reduction*

The procedures for the geometric and photometric calibration of data of this kind are now routine. Detailed descriptions of the steps involved have been given by Davies (1981) and Kormendy and Illingworth (1982). Here we outline the reduction procedure and distinguish the data sets, IPCS or HGVS, only where differences arise.

The primary step in the photometric calibration is division of the data by flat-field spectra that have been normalized to the slit response using a blank-field sky spectrum. Since the HGVS data are output in analog form, a bias frame must be first subtracted from all data frames. Geometrical rectification was carried out by fitting polynominals to the comparison arc lines and then using the resulting map to remove the distortion by rebinning the data. The velocity residuals were 5–10 km s^{-1}. The S-distortion in the HGVS was mapped by tracing the peak of the galaxy light and was removed by a further interpolation perpendicular to the dispersion direction. For the AAT data, the hardware control of the IPCS scan pattern made this step unnecessary. Consecutive frames of the same galaxy were summed, and a spectrum of the night sky was obtained by averaging the data at the edges of the summed frames. This sky spectrum was subtracted from the galaxy data.

d) *Analysis*

Both sets of data were analyzed using the Fourier quotient technique described by Sargent *et al.* (1977). This method has been tested extensively by several authors (Schechter and Gunn 1979; Efstathiou, Ellis, and Carter 1980; Kormendy and Illingworth 1982); it is known to be relatively insensitive to the spectral type of the template star and to reproduce velocity dispersions accurately down to the width of the instrumental profile.

The usual steps were taken to prepare the data for analysis by the Fourier quotient method. In particular, the data were binned onto a logarithmic wavelength scale, and continuum trends were removed by fitting and subtracting a low-order polynominal. The ends of the spectra were tapered by a cosine bell, and night-sky emission features were removed (5577 Å for the IPCS and 4358 Å for the HGVS data). As required for the Fourier method, the spectra of the template stars had high signal-to-noise ratios (i.e., $S/N \gtrsim 50$ pixel^{-1}). The IPCS template was a composite of four stellar spectra added after applying a shift so that no significant broadening was introduced. Stable fits to the Fourier quotient were obtained by fitting over the wavenumber range $10 \leq k \leq 300$ (150 for the HGVS). Hβ was particularly strong in the spectrum of NGC 4742. These data were analyzed with and without this feature, and the

TABLE 2A

GALAXY OBSERVATIONS

NGC	TYPE RC2	TYPE RSA	TYPE UGC/ESO	POSITION ANGLE (deg)	EXPOSURE (s)
2778[a]	...	...	E	40	5000
3605[a]	E4	E5	E–S0	17	7200
3818	E5	E5	...	100	10650
3904	E2	E2	E	8	7200
4387[a]	E5	...	E	140	4000
4478	E2	E2	E	140	9600
4551[a]	E3	...	E	70	4000
4742	E4	E4	...	75	8700
5638	E1	E1	E	150	7800
5831	E3	E4	E	145	7200
5845	E3	...	E	150	9450
3136	E4	E4	E	25	1000
3605	E4	E5	E–S0	4	1000
3608	E2	E1	E	75	1000
3923	E4	E4/S0$_1$(4)	E	13	1000
3962	E1	E1	...	13	1000
4458	E0	...	E	175	1500
4489	E1	...	E	4	1200

[a] Observed at KPNO.

TABLE 2B

TEMPLATE STAR OBSERVATIONS

Star	m_V	Spectral Type	Exposure[a] (s)	Dispersion (Å mm^{-1})
HD 90518	6.1	K1 III	2000	33
HD 144046	6.0	G9 III	1200	33
HD 154779	6.1	K0 III	1000	33
HD 155500	6.1	K0 III	2500	33
HD 52071[b]	7.2	K2 III	400	25/50
HD 56224[b]	7.4	K1 III	400	25/50
HD 85990[b]	8.0	K0 III	400	50
HD 143393[b]	7.1	K3 III	400	25

[a] 7.5 mag neutral density used at AAT, 2.5 mag KPNO.
[b] Observed at KPNO.

results were found to be in close agreement. The center of this galaxy was also bright enough to saturate the IPCS. In severe cases, this can lead to an overestimate of the velocity dispersion (Davies 1979). A short exposure of the spectrum of NGC 4742 was therefore taken through a 1.75 mag neutral density filter and analyzed separately to give the central dispersion. A comparison of the results, 116 ± 11 km s^{-1} for the 7200 s integration and 110 ± 14 km s^{-1} for the 1500 s integration showed that the effects of saturation were negligible in this case.

The IPCS data were also analyzed using the cross-correlation method of Tonry and Davis (1980), and the results were found to be in excellent agreement with those from the Fourier quotient method. The two techniques gave velocities with an rms difference of 5 km s^{-1} and dispersions with an rms difference of 9 km s^{-1}, smaller than the formal errors in both cases. Since tests with artificially broadened template spectra showed that the velocity dispersions from the Fourier quotient method are more reliable than those from the cross-correlation method when $\sigma \leq 60$ km s^{-1}, we have presented results only for the Fourier quotient method. The errors for these data are, however, taken from the cross-correlation method. Our experience is that these are generally smaller than the errors derived from the Fourier quotient method, which tends to overestimate the uncertainties as judged from point-to-point scatter in the profiles. As a check on the internal consistency of our measurements, one galaxy, NGC 3605, was observed both at KPNO and at the AAT (a short exposure giving only the central dispersion). The agreement between these measurements is excellent: $\sigma_{\rm HGVS} = 93 \pm 3$ km s^{-1} and $\sigma_{\rm IPCS} = 90 \pm 9$ km s^{-1}.

e) Results

The folded rotation curves and dispersion profiles of the galaxies with long exposures are plotted in Figures 1*a* and 1*b*, and the results are tabulated in the Appendix. In most cases, the data extend out to the effective radius of each galaxy, with relative errors that increase from

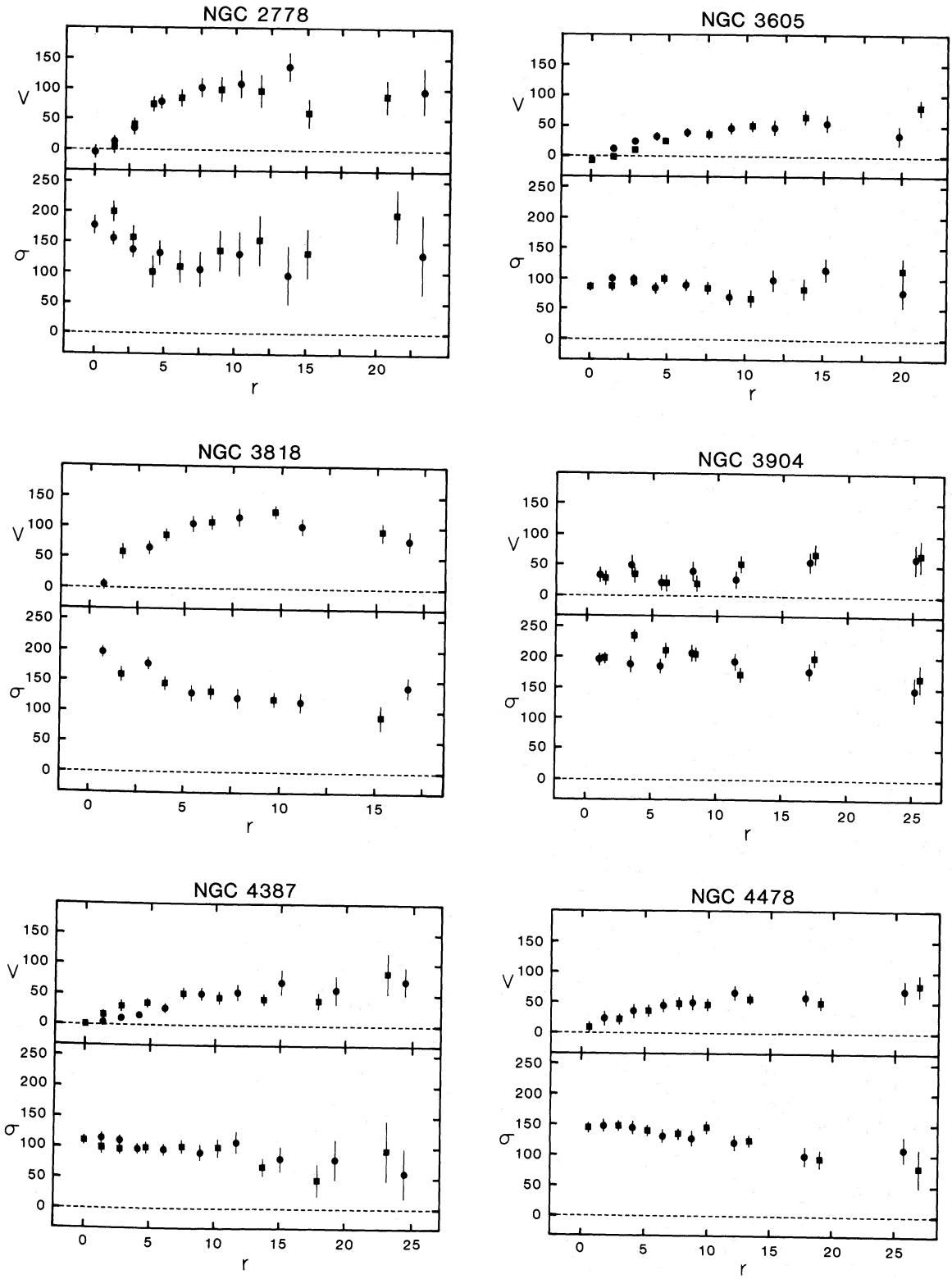

FIG. 1a

FIG. 1.—(*a*) Rotation velocities V and velocity dispersions, σ, both in km s^{-1}, plotted against radius, r, in arc seconds, along the major axis. All the data are folded with different sides being represented by filled circles or filled squares. (*b*) Same as (*a*).

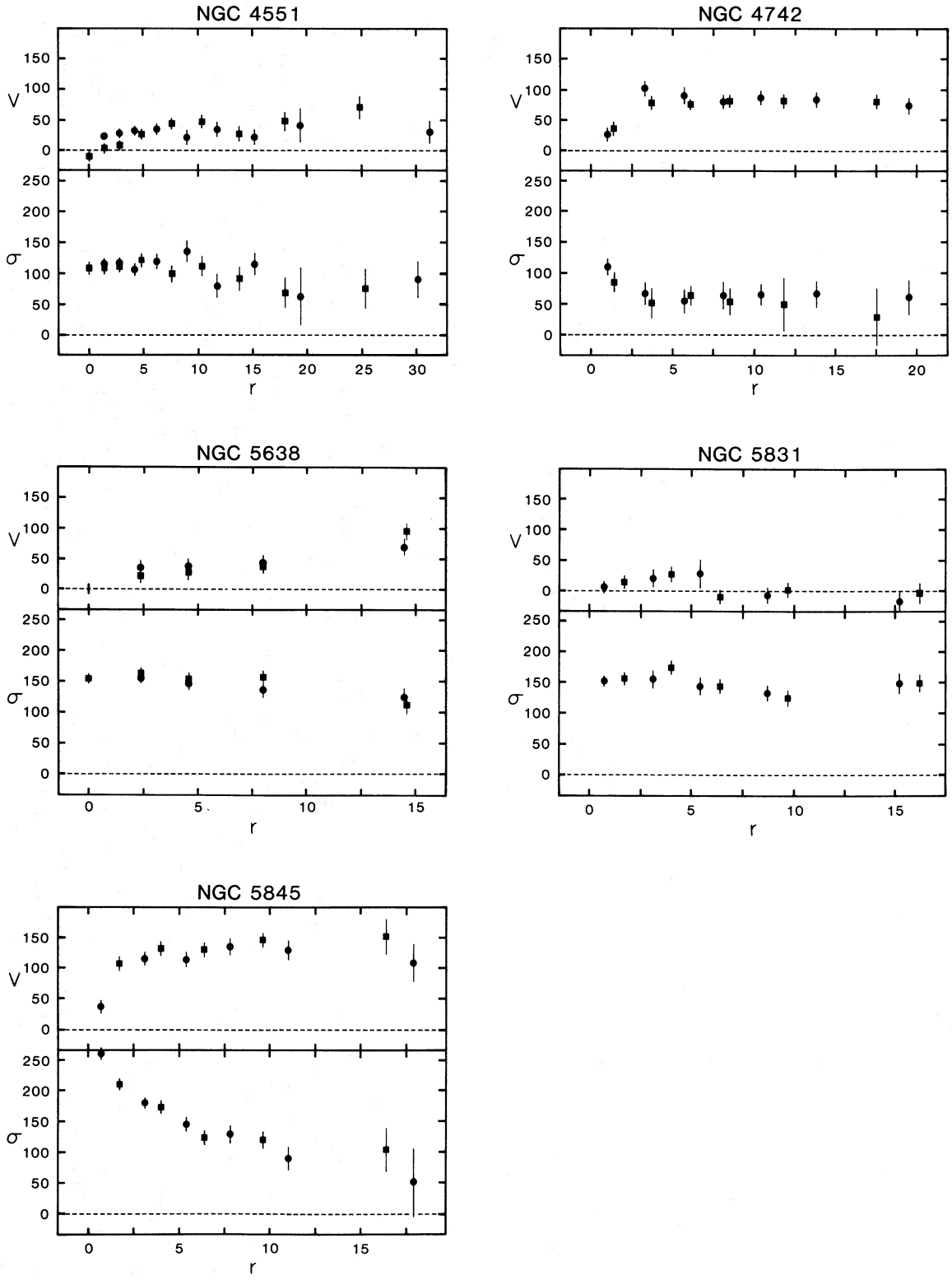

FIG. 1*b*

TABLE 3

COMPILATION OF DATA FOR ELLIPTICAL GALAXIES AND BULGES

NGC	Group	cz	ε	r_e	V_m	σ_0	$\bar{\sigma}$	Ref.	$-M_B^{UH}$	$-M_B^{VF}$	$V_m/\bar{\sigma}$	$(V/\bar{\sigma})^*$
(1)	(2)	(3)	(4)	(5)	(6)	(7)	(8)	(9)	(10)	(11)	(12)	(13)
315	...	5128	0.31	32:	$\leq$30	314±26	311±11	17,18	23.08	21.88	$\leq$0.10	$\leq$0.15
584	584	1960	0.37	27	159±8	230±12	168±6	4,14,18	21.81	20.49	0.95	1.25
596	584	1960	0.37	30	73±16:	165±11	143±14	14,17,20	21.24	19.92	0.51	0.67
720	...	1820	0.37	38	76±12	239±8	214±11	14,16,17	21.70	20.39	0.36	0.47
1052	1084	1458	0.31	30	96±5	245±7	207±13	17	20.87	19.59	0.46	0.70
1600	1600	4587	0.26	34	$\leq$30	332±12	304±17	17	22.90	21.74	$\leq$0.10	$\leq$0.17
1700	1700	3883	0.29	27	74±30:	251±10	256±10	17,18	22.77	21.62	0.29	0.46
2768	2768	1450	0.56^{+L}	60	102±8	218±23	187±11	11,18	21.50	20.81	0.55	0.48
2778	...	1984	$0.29^{N/E}$	(17)	99±7	178±13	141±10	this work	20.33	19.57	0.70	1.11
3136	...	1423	0.32	25	...	238±18	...	this work	(20.97)	(20.11)	...	...
3377	dV11	716	0.37^{+L}	42	80±6	152±17	131±8	11,18,19	19.76	18.39	0.61	0.80
3379	dV11	716	0.13^{+L}	56	43±11	231±5	184±9	3,4,9,15 16,18,19	20.62	19.25	0.23	0.61
3557	3557	2707	0.32	42	178±20	222±16	(253±20)	3,11	22.56	21.68	0.70	1.03
3605	dV49	870	0.41	17:	52±5	91±4	90±3	this work	18.16	17.96^{+}	0.58	0.70
3608	dV49	870	0.19	27	...	181±15	...	this work	19.32	19.12^{+}	...	...
3818	dV23	1553	0.32	19	114±7	196±7	151±10	this work	19.83	19.39	0.75	1.11
3904	dV44	1640	0.26	19	63±3	197±6	203±5	this work	20.77	20.21	0.31	0.57
3923	dV44	1640	0.35.	30	...	249±9	...	this work	21.62	21.06	...	...
3962	dV23	1553	0.09	29:	...	234±28	...	this work	20.98	20.55	...	...
4278	dV13	972	0.07^{+L}	30	50±10	243±8	244±28	17,18	20.30	19.76^{+}	0.20	0.78
4365	Virgo	1019	0.25^{+L}	53	15±15	264±8	247±16	11,18	20.94	20.37	0.06	0.10
4374	Virgo	1019	$0.10^{+L,K}$	53	$\leq$38	298±6	261±22	3,9,14,16 18,19	21.24	20.67	$\leq$0.15	$\leq$0.45
4387	Virgo	1019	0.38	15	57±5	111±7	102±3	this work	18.60	18.03	0.56	0.72
4406	Virgo	1019	$0.24^{+L,K}$	70	31±16	253±7	244±6	3,14,16,18	21.44	20.87	0.13	0.22
4458	Virgo	1019	0.05	21	...	100±12	...	this work	18.65	18.08	...	...
4472	Virgo	1019	$0.18^{+L,K}$	99	44±10	310±7	256±18	3,7,9,10 13,16,18,19	22.23	21.67	0.17	0.37
4473	Virgo	1019	0.42^{+L}	36	60±3	180±10	183±3	18,21	20.52	19.95	0.33	0.39
4478	Virgo	1019	0.15^{+L}	15	62±4	145±7	142±4	this work	19.42	18.85	0.44	1.05
4486	Virgo	1019	$0.14^{+L,K}$	95	$\leq$20	336±7	303±10	6,9,10 15,16,18	21.99	21.42	$\leq$0.07	$\leq$0.18
4489	Virgo	1019	0.05	22:	...	53±15	...	this work	18.68	18.11	...	...
4551	Virgo	1019	0.19	16	38±5	110±5	114±3	this work	18.70	18.13	0.33	0.69
4621	Virgo	1019	$0.34^{+L,K}$	42	65±10	227±11	...	13,16,18	20.80	20.23	...	...
4636	Virgo	1019	0.19^{+K}	67	79±30	227±12	189±28	3,16,18	21.04	20.48^{+}	0.42	0.88
4649	Virgo	1019	0.19^{+K}	67	60±9	361±12	305±21	10,11,13 16,18	21.72	21.15	0.20	0.41
4697	Virgo	1019	0.38^{+K}	67	103±3	181±6	161±11	1,3,4,16	21.34	20.78^{+}	0.64	0.82
4742	Virgo	1019	0.34	23:	83±2	110±14	67±6	this work	19.44	18.88^{+}	1.24	1.74
4839	Coma	6967	0.50	42:	16±10	269±25	(244±18)	4	23.17	22.16	0.07	0.07
4889	Coma	6967	0.31	36	24±19	354±33	(362±22)	4	23.39	22.37	0.07	0.11
5638	5566	1583	0.09	24	62±13:	154±8	152±3	this work	20.36	19.85	0.41	1.31
5813	dV50	1557	0.25^{+L}	44	8±2	225±6	219±3	7,8	20.85	20.32	0.04	0.07
5831	dV50	1557	0.09	27	27±9	152±9	148±5	this work	20.09	19.56	0.18	0.58
5845	dV50	1557	0.35	8:	127±5	263±8	194±20	this work	19.43	18.90	0.65	0.89
6909	...	2610	0.48	23:	28±4	112±6	114±4	4	20.99	20.01	0.25	0.26
7562	7619	3820	0.29	21	$\leq$40	274±29	241±12	17,18	21.87	20.64	$\leq$0.17	$\leq$0.27
7619	7619	3820	0.09	30	65±14	354±18	298±18	17	22.39	21.15	0.21	0.70
7626	7619	3820	0.17	34	$\leq$30	270±14	324±24	14,16,17,18	22.23	20.99	$\leq$0.09	$\leq$0.21
7785	...	4020	0.40	22	100±17:	240±17	233±9	17,18	22.03	20.79	0.43	0.53
I2082	...	11850	0.33^{C}	19	<31	268±17	230±16	2	23.25	22.10	$\leq$0.13	$\leq$0.19
I4296	...	3619	0.10^{EEC}	48	64±12:	300±9	291±11	7	22.94	21.99	0.22	0.67
A2029	A2029	23310	0.33^{D}	(15)	<20	375±10	369±5	5	23.42	22.32	$\leq$0.05	$\leq$0.08
224	...	...	0.25	...	65±15	152±9	145±13	12	18.57	18.57	0.45	0.78
1553	dV16	934	0.42	...	156±5	195±10	170±10	12	19.19	18.46	0.92	1.08
3031	...	...	0.33	...	100±5	159±9	146±9	12	18.70	18.70	0.68	0.97
3115	...	476	0.57	...	195±20	246±17	184±20	12	19.74	19.78	1.06	0.92
4565	dV13	972	0.41	...	100±13	150±10	138±11	12	20.00	19.54	0.72	0.86
4594	Virgo	1019	0.37	...	130±24	256±22	207±14	12	22.18	21.71	0.63	0.82
5866	dV30	930	0.53	...	132±17	170±11	152±11	12	20.42	20.00	0.87	0.82
7814	7814	1140	0.47	...	123±12	167±18	144±10	12	20.39	19.31	0.85	0.90

about 5% in the center to about 15%–30% in the outer parts. The central velocity dispersions of the six galaxies with short exposures are listed in Table 3 (see § III). These values are the luminosity-weighted dispersions from the central four to five scan lines of IPCS data, which correspond to effective apertures of 9″–12″. For these, the velocity dispersions are accurate to about 10%.

Of the many measurements of central velocity dispersions, those of Tonry and Davis (1981*a*, *b*) and Tonry (1981) have the greatest overlap with our sample. To compare our results with theirs, we have derived luminosity-weighted dispersions that correspond to their aperture of 3″ × 12″. These values are plotted against the Tonry-Davis values in Figure 2. The mean difference between our measurements and the recent measurements by Tonry (1981), which were taken with high spectral resolution, is only 14 km s^{-1}, but the results from the earlier work of Tonry and Davis (1981*a*, *b*) are systematically high by 27 km s^{-1}. This is probably due to the low spectral resolution used in the earlier study. Another possibility is that some of this bias may be due to a rotational contribution to the broadening since the aperture used by Tonry and Davis was always aligned E-W rather than along the minor axis.

The rotation curves and dispersion profiles of the faint ellipticals share the diversity of forms seen in bright ellipticals. Several of the galaxies in our sample have dispersion profiles that fall rapidly from the center. Particularly noteworthy is NGC 5845, where the velocity dispersion drops by a factor of 2 in the central few arc seconds, and the rotation curve shows a steep rise. The detailed forms of the dispersion profiles and rotation curves will be interpreted in conjunction with surface photometry in a future paper. Emphasis is given in the present paper to the global properties of these galaxies; the most important features of the data are therefore the maximum rotation velocity and the velocity dispersion in the inner parts of each galaxy.

III. KINEMATIC RELATIONS

a) Compilation of Available Data

To examine the kinematic properties of ellipticals and bulges as a function of luminosity, we have compiled data that were analyzed with Fourier transform techniques. They are presented in a uniform way in Table 3. The sample includes the 17 galaxies that we observed, the 8 bulges studied by Kormendy and Illingworth (1982), and 33 ellipticals from the literature. Of the ellipticals, two are cD type; the remainder appear to be "normal," and none is as faint as the dwarfs of the Local Group. The sample is well populated over two decades in luminosity, from $M_B \approx -18.5$ to $M_B \approx -23.5$.

The maximum rotation velocity of each galaxy, V_m, is given in column (6) of Table 3. These values have been estimated from the figures and tables in the sources listed in column (9) and are generally accurate to better than 20%. The rotation curves of most ellipticals peak or flatten at radii between 0.1 and 0.5 effective radii, r_e. In a few galaxies, however, the rotation curve increases to the outermost point observed. In these cases, which are indicated by colons, the maximum rotation velocity is less certain but has been taken to be the average velocity of the outer few points.

Two values of velocity dispersion are listed in Table 3: σ_0, in column (7), is the average of published central velocity dispersions, and $\bar{\sigma}$, in column (8), is the unweighted average value of the dispersions within $\frac{1}{2}r_e$ taken from the references in column (9). The central velocity dispersions have often been measured several times and are generally accurate to better than 10%. These values

---

NOTES.—Each of the following notes is numbered to correspond to the column in Table 3 for which it provides further explanation and information. (1) Galaxy identification: by NGC number, IC number (I), or in the case of the cD galaxy studied by Dressler (1979), the Abell cluster number (A). (2) Group assignment: by de Vaucouleurs 1975 group number or by the brightest member. (3) Adopted group velocity in km s^{-1}. (4) Ellipticity: taken to be $\epsilon = 1 - R_{25}^{-1}$ from the RC2, or when superscripts +L and +K appear, the RC2 value was averaged with the ellipticity at r_e from King 1978 or Leach 1981. Other sources of ellipticities: N/E, Nilson 1973 or ESO/Uppsala catalog; C, Carter *et al.* 1981; EEC, Efstathiou, Ellis, and Carter 1980; D, estimated from the isophotes plotted in Dressler 1978. (5) Effective radius (in arcsec): taken to be $A_e/2$ when A_e was available from the RC2. For those galaxies marked with a colon, r_e was taken to be $D_{25}/6$. For NGC 2778, r_e was calculated from the major axis diameter given in the UGC as described in the RC2. For A2029, r_e was estimated from the surface brightness profile given in Dressler 1979. Uncertain values are enclosed in parentheses. (6) Maximum rotation velocity (in km s^{-1}): colons indicate those galaxies with rotation curves that continue to rise to the outermost radius measured. (7) Central velocity dispersion (in km s^{-1}): the average of values from the sources referenced in col. (9). (8) Average velocity dispersion within $\frac{1}{2}r_e$ (in km s^{-1}). (9) References for kinematic data given in cols. (6), (7), and (8) are provided below. (10) Absolute magnitudes calculated from B_T magnitudes in the RC2 (or corrected Harvard magnitudes when B_T was not available) on the basis of a uniform Hubble flow with $H_0 = 50$ km s^{-1} Mpc^{-1}. Magnitudes for NGC 3115, 2778, and 4489 were taken from the catalog of Zwicky *et al.* 1961–1968 and corrected to the B_T system as described by de Vaucouleurs and Pence 1979. The magnitude for NGC 3136 is marked as uncertain because of the large extinction correction. The magnitude for the cD galaxy in A2029 was taken from Sandage 1973. The magnitudes given for the disk galaxies studied by Kormendy and Illingworth 1982 are *bulge* magnitudes. (11) As for col. (10), except that distances were calculated from the Virgocentric flow model given by eq. (2) of Schechter 1980 with $\gamma = 2$ and an infall velocity of 300 km s^{-1} (see § III*a*). Galaxies marked (+) have triple valued distances; the intermediate solutions are tabulated. (12) Ratio of the maximum rotation velocity to the average velocity dispersion within $r_e/2$. (13) $V_m/\bar{\sigma}$ from col. (12) divided by the value of V/σ expected from models having oblate figures with the observed ellipticities and isotropic residual velocities (see § III*a*).

REFERENCES.—(1) Bertola and Capaccioli 1975; (2) Carter *et al.* 1981; (3) Davies 1981; (4) Davies and Illingworth 1983; (5) Dressler 1979; (6) Dressler 1980*a*; (7) Efstathiou, Ellis, and Carter 1980; (8) Efstathiou, Ellis, and Carter 1982; (9) Malamuth and Kirshner 1981; (10) Faber and Jackson 1976; (11) Illingworth 1977; (12) Illingworth and Schechter 1982; Kormendy and Illingworth 1982; (13) Peterson 1978; (14) Sargent *et al.* 1977; (15) Sargent *et al.* 1978; (16) Schechter 1980; (17) Schechter and Gunn 1979; (18) Tonry and Davis 1981*a*; (19) Whitmore, Kirshner, and Schechter 1979; (20) Williams 1979; (21) Young *et al.* 1978.

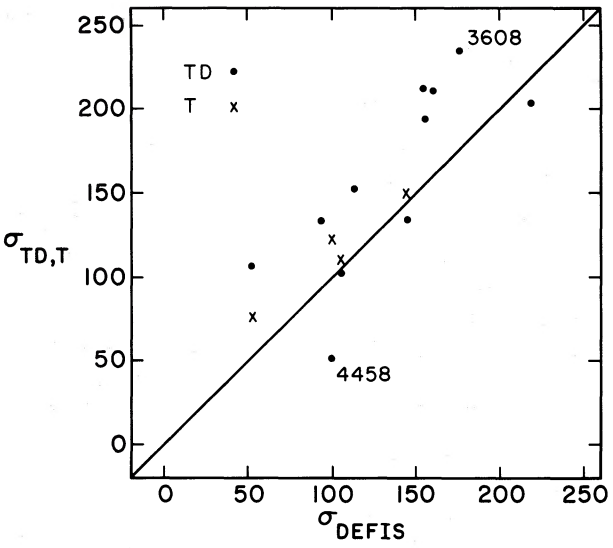

FIG. 2.—Velocity dispersions from this paper plotted against those of Tonry and Davis (1981*a*, *b*) and Tonry (1981).

may be influenced by the presence of a central mass concentration or velocity anisotropy, and we therefore consider $\bar{\sigma}$ to be a more representative dispersion. As expected, $\bar{\sigma}$ is usually smaller than σ_0, but only in a few cases does the difference exceed 20%.

Estimates of the effective radii, r_e, for the ellipticals are given in arc seconds in column (5) of Table 3. The values of the r_e for the majority of galaxies in the sample were calculated from the effective diameters, A_e, in the RC2, which were determined from multiaperture photoelectric photometry or detailed photographic photometry. For seven galaxies, A_e was not given, and so we have taken $r_e = \frac{1}{6}D_{25}$, where D_{25} is the diameter at the $B = 25$ mag arcsec^{-2} isophote. A comparison of the two estimates of the r_e for the majority of galaxies in our sample shows that this procedure leads to no systematic bias and an rms scatter of only 17%.

For comparison with theoretical models, it is preferable to have measurements of ellipticity and kinematics in the same part of a galaxy. Ellipticities at the appropriate radii are available for only 16 of the galaxies in our sample from the studies of King (1978) and Leach (1981). We have compared their ellipticities at r_e with those at $\frac{1}{2}D_{25}$ ($\sim 3r_e$) from the RC2 and find no systematic difference. Except when noted, the ellipticities given in column (4) of Table 3 are those from the RC2 or are averages of the RC2 values and the Leach and King values at r_e. In individual cases, these estimates may not reflect the ellipticity in the central regions of a galaxy, but they should be appropriate for the sample as a whole.

To estimate absolute magnitudes, we have assigned the galaxies to groups and have used the mean velocity of each group as a distance indicator. The name of the group and the adopted group velocity are given in columns (2) and (3) of Table 3. Group membership was determined from de Vaucouleurs (1975), from our inspection of the Palomar and ESO sky surveys, and from recession velocities in the lists of Tonry and Davis (1981*a*,*b*), Rood (1981), Sandage and Visvanathan (1978), Sandage (1978), and the RC2. Apparent magnitudes, on the B_T system, were taken from the RC2. One set of absolute magnitudes, M_B^{UH}, given in column (10) of Table 3, was derived assuming a uniform Hubble flow with $H_0 = 50$ km s^{-1} Mpc^{-1}. Another set of magnitudes, M_B^{VF}, given in column (11), was derived using a model of the Virgocentric flow, equation (2) in Schechter (1980) with $\gamma = 2$, and an infall velocity of 300 km s^{-1}. The distance modulus and center of the Virgo Cluster were taken to be 30.98 (Mould, Aaronson, and Huchra 1980) and $\alpha(1950) = 12^h27^m.6$, $\delta(1950) = 12°56'$. In this case, the far-field Hubble constant is $H_0 = 84$ km s^{-1} Mpc^{-1}. Entries marked with plus signs have triple-valued distances on the inflow model, and only the intermediate solutions are tabulated. An extinction correction of 0.13 ($\csc|b| - 1$) and a K-correction of $5.32z$ have been applied to both sets of magnitudes.

b) *Relation between Rotation and Luminosity*

In Figure 3 we have plotted $V_m/\bar{\sigma}$ against ellipticity. The filled circles show ellipticals fainter than $M_B^{UH} = -20.5$ and the open circles show the brighter galaxies. It is clear that the faint ellipticals rotate more rapidly than most of the bright ellipticals. Also shown in this diagram is the relationship derived from the tensor virial theorem under the assumption that ellipticals are oblate spheroids of constant ellipticity with isotropic velocity distributions (Binney 1978). The predicted ratio, $(V/\sigma)_{OI}$, follows if the rotation curve and dispersion profile are

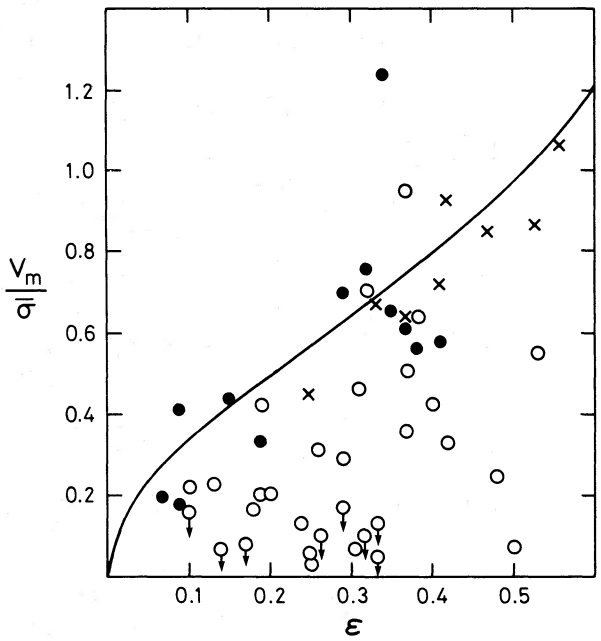

FIG. 3.—The quantity $V_m/\bar{\sigma}$ against ellipticity. Ellipticals with $M_B^{UH} > -20.5$ are shown as filled circles; ellipticals with $M_B^{UH} < -20.5$, as open circles; and the bulges of disk galaxies, as crosses. The solid line shows the $(V/\sigma, \epsilon)$-relation for oblate galaxies with isotropic velocity dispersions (Binney 1978).

assumed to be flat. From a more detailed study of oblate isotropic models (Binney 1980), we would expect $(V_m/\bar{\sigma})$ to be nearly equal to $(V/\sigma)_{OI}$. Furthermore, projection does not affect the comparison with the oblate isotropic model for galaxies rounder than E5. Thus, if the faint ellipticals conformed to this model, one would expect the observed values of $V_m/\bar{\sigma}$ to lie close to the theoretical line, as is the case. (The exception is NGC 4742 for which $V_m/\bar{\sigma}$ lies far above the line for oblate isotropic models; see the discussion below.) If, however, the faint galaxies were prolate with isotropic velocity dispersions, one would expect a large scatter in $V_m/\bar{\sigma}$ at any given ellipticity (Binney 1978). Hence our results suggests that the faint ellipticals have nearly oblate figures.

For each galaxy we have calculated the quantity $(V/\sigma)^*$, which is defined to be the ratio of the observed value of $V_m/\bar{\sigma}$ to $(V/\sigma)_{OI}$. This ratio is useful because it is approximately equal to unity for oblate isotropic galaxies, independent of ellipticity and projection effects. We have plotted log $(V/\sigma)^*$ against absolute magnitude in Figure 4. There is a definite correlation, showing that faint ellipticals rotate more rapidly than bright ellipticals. The Spearman rank correlation coefficient for these data shows that we can reject the hypothesis that $(V/\sigma)^*$ is not correlated with absolute magnitude at the $\ll 0.1\%$ level of significance. (We treat the upper limits as detections throughout this section.) There is a large spread in $(V/\sigma)^*$, especially for the bright galaxies. It is extremely unlikely that all of the observed scatter is due to observational errors. Unlike most bright ellipticals, NGC 3557 and NGC 4697 are definitely rapid rotators. The scatter for the bright galaxies is therefore probably due to a combination of varying degrees of anisotropy and to projection effects.

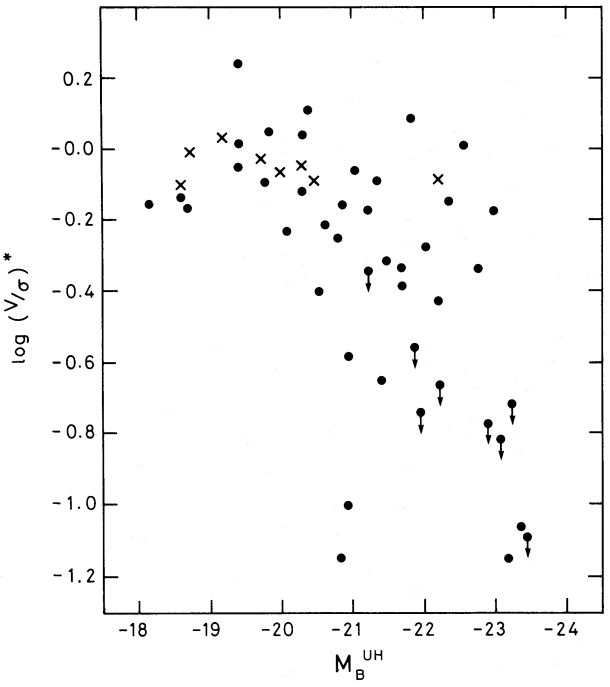

FIG. 4.—Log $(V/\sigma)^*$ against absolute magnitude. Ellipticals are shown as filled circles and the bulges as crosses; $(V/\sigma)^*$ is defined in § III*b*.

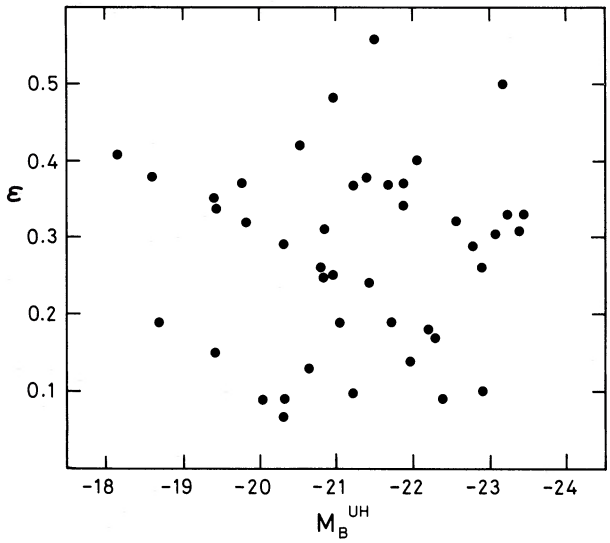

FIG. 5.—Ellipticity against absolute magnitude, for elliptical galaxies with measured rotation curves.

The quantity of most interest in the comparison with theories of galaxy formation is the dimensionless spin parameter,

$$\lambda = J|E|^{1/2}G^{-1}M^{-5/2}, \quad (1)$$

where J, E, and M are the total angular momentum, energy, and mass of the galaxy respectively. This is related to $V_m/\bar{\sigma}$ according to $\lambda \approx 0.3(V_m/\bar{\sigma})$ for an oblate, Hubble-like galaxy viewed along the equatorial plane (White 1979). Averaging over random orientations, the mean value of $V_m/\bar{\sigma}$ should be multiplied by $4/\pi$ in order to obtain the mean value of λ. As Figure 5 shows, there is no correlation between ellipticity and absolute magnitude in this sample. The dependence of $V_m/\bar{\sigma}$ on luminosity should therefore give an unbiased measure of the dependence of λ on luminosity. In Figure 6 we plot log $(V_m/\bar{\sigma})$ against absolute magnitude. A least squares fit, minimizing residuals in log $(V_m/\bar{\sigma})$, gives

$$\log (V_m/\bar{\sigma}) = (0.155 \pm 0.04)M_B^{UH} + (2.7 \pm 0.8), \quad (2)$$

over the range $-18 \geq M_B^{UH} \geq -23.5$. This is shown as the solid line in Figure 6. We emphasize that the scatter in the data points is very large, and it is by no means clear that a power law is an accurate representation of the true relation. From Figure 3 and the distributions of apparent ellipticities presented by Sandage, Freeman, and Stokes (1970) for a random sample of ellipticals we estimate that this relation is biased upward by at most 0.1 in log $(V_m/\bar{\sigma})$ as a result of the preference for flattened ellipticals in kinematic studies.

There appear to be no selection effects that could be responsible for a spurious correlation. The most serious possibility is that some of the faint galaxies might be

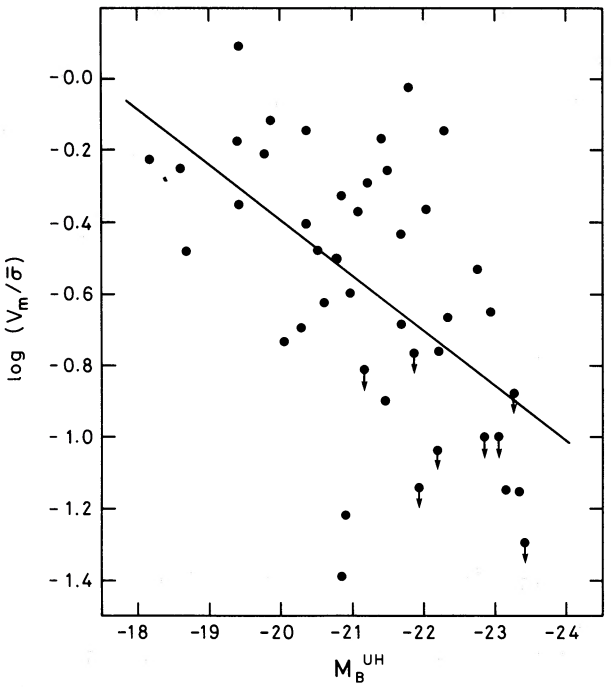

FIG. 6.—Log $V_m/\bar{\sigma}$ for ellipticals against absolute magnitude. The solid line shows the least square power-law fit given by eq. (2).

misclassified lenticular galaxies. None of the galaxies that we observed with a long exposure is classified as an S0 in any of the major catalogs. The main uncertainty is for NGC 3605, which is classified as E-S0 in the UGC, although it is classified as an elliptical galaxy in both the RC2 and the RSA. For four faint galaxies, however, the velocity dispersion profiles fall steeply, possibly implying the presence of a disk component. These are NGC 4742, 5845, 3818, and 2778 (in order of increasing $\bar{\sigma}/\sigma_0$). In particular, NGC 4742 rotates much more rapidly than expected on the oblate isotropic model, and we therefore suspect that this galaxy is an S0. The question of whether any of the other galaxies in our sample are lenticular galaxies will only be resolved by detailed photometric and kinematic studies. Even if these four galaxies are excluded from the sample, our conclusions remain unchanged. The Spearman rank correlation coefficient still rejects the hypothesis of no correlation between $(V/\sigma)^*$ and absolute magnitude at the 0.1% level of significance.

c) *Comparison with Bulges of Disk Galaxies*

The results for the eight bulges studied by Illingworth and Schechter (1982) and Kormendy and Illingworth (1982) are given at the foot of Table 3. As in the latter reference, V_m is the maximum rotation velocity corrected to the major axis from offset spectra and $\bar{\sigma}$ is again the mean dispersion within $\frac{1}{2}r_e$. Thus the $V_m/\bar{\sigma}$ values for bulges can be compared directly with those for the ellipticals. The main difference in the comparison is in the choice of ellipticity. For the bulges, the ellipticities are means over the range in radii for which the rotation curves were obtained. As Figure 3 shows, the bulges in the present sample are, on average, flatter than the ellipticals. This is to be expected as the disk galaxies, and therefore the bulges, were chosen to be edge on, whereas the ellipticals occur at random orientations. Projection does not affect the comparison with the oblate isotropic model, so our conclusions are not affected by this bias. As Figure 4 shows, there is no statistically significant difference between the values of $(V/\sigma)^*$ for bulges and ellipticals with similar absolute magnitudes. Both faint ellipticals and bulges rotate more rapidly than bright ellipticals.

It would be interesting to know whether the bulges also show a trend between rotation and luminosity. Unfortunately, there are not enough bulges in the present sample to test for this. We note, however, that the bulge of the Sombrero galaxy (NGC 4594) is 1.8 mag brighter than the others and that it rotates more rapidly than most ellipticals of the same absolute magnitude. Further observations of very luminous bulges are necessary to test for a dependence of their rotational properties on luminosity.

d) *Relation between Central Velocity Dispersion and Luminosity*

An additional aim of this project was to investigate the relation between central velocity dispersion and luminosity, and in particular the behavior at low luminosities. Previous investigators have found $L \propto \sigma_0^n$ with $n \approx 4$ (Faber and Jackson 1976; Tonry and Davis 1981*a*; Terlevich *et al.* 1981, and references therein). However, only a few galaxies with $M_B > -20$ in these studies have accurately measured velocity dispersions (see the discussion in § II*d*).

In Figure 7*a* we have plotted $\log \sigma_0$ against M_B^{UH} for all the ellipticals in Table 3. A least squares fit, minimizing residuals in $\log \sigma_0$, gives a slope of $n = 3.9 \pm 0.4$. There is a scatter of 0.8 mag in Figure 7*a*, and, when the residuals in M_B^{UH} are minimized, a slope of $n = 2.5 \pm 0.3$ is found. As a result of the large difference between these fits, the true value of n is difficult to determine. For the purposes of this discussion, we quote only the fits that minimize residuals in $\log \sigma_0$; details of the fits in both directions and the errors are given in Table 4.

Figure 7*a* gives the impression that the relation between luminosity and velocity dispersion flattens at high luminosities. As Figure 7*b* shows, the effect is reduced when magnitudes from the Virgocentric flow model are used. By splitting the sample at $M_B^{VF} = -20$, we have examined whether this relation is different for bright and faint galaxies. For the 30 brighter galaxies in Figure 7*b*, the slope is $n = 4.2 \pm 0.9$, and, for the 14 fainter galaxies, the slope is $n = 2.4 \pm 0.9$. This marginally significant difference suggests that the relation between velocity dispersion and luminosity steepens at low luminosities.

Tonry (1981) has recently measured velocity dispersions for a complete sample of ellipticals in the core of the Virgo Cluster. He finds a slope $n = 3.2 \pm 0.2$ over the entire range in absolute magnitude with a scatter of

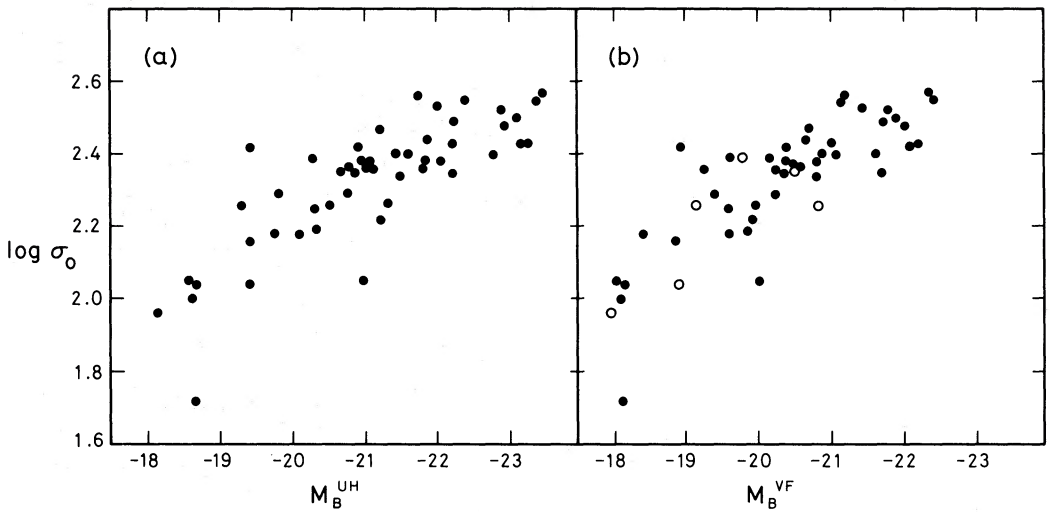

FIG. 7.—(*a*) Log σ_0 against absolute magnitude, M_B^{UH}, derived on the assumption of a uniform Hubble flow, for the ellipticals listed in Table 3. (*b*) Log σ_0 against absolute magnitude, M_B^{VF}, derived from the Virgocentric flow model discussed in § III*a*. The open circles show those galaxies with triple-valued distances on the inflow model. These have been plotted at the absolute magnitudes corresponding to the intermediate solution.

only 0.4 mag. He excluded from the fit the two galaxies with the lowest velocity dispersions, NGC 4239 and NGC 4489, because the measurements were uncertain. However, our data for NGC 4489 give an even lower velocity dispersion with similar uncertainty. By including the two faint galaxies in the fit, the value of n is decreased and the scatter at low luminosities is increased. In this respect, our findings are consistent with those of Tonry to within the uncertainties of small samples.

There is some indication for a difference in the amplitude of the L-σ^n relation between galaxies in the Virgo Cluster and those outside. If we constrain n to be 3.2 and exclude Virgo galaxies, we find $\sigma_{11} = 177 \pm 8$ km s^{-1} (where σ_{11} is the velocity dispersion from the fitted relation for a galaxy with $B_T = 11.0$ at the distance of Virgo). This is substantially smaller than the value, $\sigma_{11} = 237 \pm 6$ km s^{-1}, deduced from the Tonry (1981) data for galaxies in the Virgo Cluster core. Using our Virgo flow model, we obtain $\sigma_{11} = 194 \pm 8$ km s^{-1}, reducing the difference slightly. These results suggest that the L-σ^n relation may be dependent on environment or on cluster morphology, and this is worth further investigation.

e) Relation between Effective Radius and Luminosity

To compare the kinematic measurements with models of galaxy formation, we require the relation between effective radius and luminosity. For our sample, the relation is shown in Figure 8. A least squares fit, minimizing residuals in log r_e, with r_e in kpc, gives

$$\log r_e = -(0.23 \pm 0.01)M_B^{UH} - (4.20 \pm 0.25) . \quad (3)$$

Only those ellipticals with A_e listed in the RC2 were included in deriving this expression. The fit is clearly very good and there is remarkably little scatter about the mean relation. Using absolute magnitudes, M_B^{VF}, derived from the Virgocentric flow model, we obtain a fit that does not differ significantly from the one above. Equation (3) implies a relation of the form $r_e \propto L^{0.58 \pm 0.03}$, which is similar to the one proposed by Fish (1964).

TABLE 4

THE LUMINOSITY-VELOCITY DISPERSION RELATION

Sample (1)	Number (2)	y (3)	x (4)	a (5)	b (6)	r (7)	$\delta\sigma$, δM (8)	n (9)
All ellipticals	50	$\log \sigma_0$	M_B^{UH}	-0.102 ± 0.01	0.166 ± 0.23	0.80	0.11	3.9
		M_B^{UH}	$\log \sigma_0$	-6.33 ± 0.7	-6.37 ± 1.6		0.83	2.5
Ellipticals with single-valued distance estimates	44	$\log \sigma_0$	M_B^{VF}	-0.114 ± 0.01	0.0197 ± 0.27	0.80	0.11	3.5
		M_B^{VF}	$\log \sigma_0$	-5.64 ± 0.6	-7.20 ± 0.5		0.74	2.3
Ellipticals with $M_B^{VF} < -20$	30	$\log \sigma_0$	M_B^{VF}	-0.095 ± 0.02	0.40 ± 0.42	0.67	0.08	4.2
		M_B^{VF}	$\log \sigma_0$	-4.67 ± 1.0	-9.79 ± 2.4		0.56	1.9
Ellipticals with $M_B^{VF} > -20$	14	$\log \sigma_0$	M_B^{VF}	-0.164 ± 0.06	-0.93 ± 0.11	0.63	0.15	2.4
		M_B^{VF}	$\log \sigma_0$	-2.45 ± 0.86	-13.6 ± 2.0		0.57	1.0

NOTE.—Least squares fits to $y = ax + b$. Col. (1) gives the sample used for the fits with the total number of galaxies given in col. (2). In col. (7), r is the correlation coefficient for the fit; $\delta\sigma$ and δM in col. (8) give the scatter of the points about the best fitting line, and n in col. (9) is the slope in the relation $L \propto \sigma_0^n$.

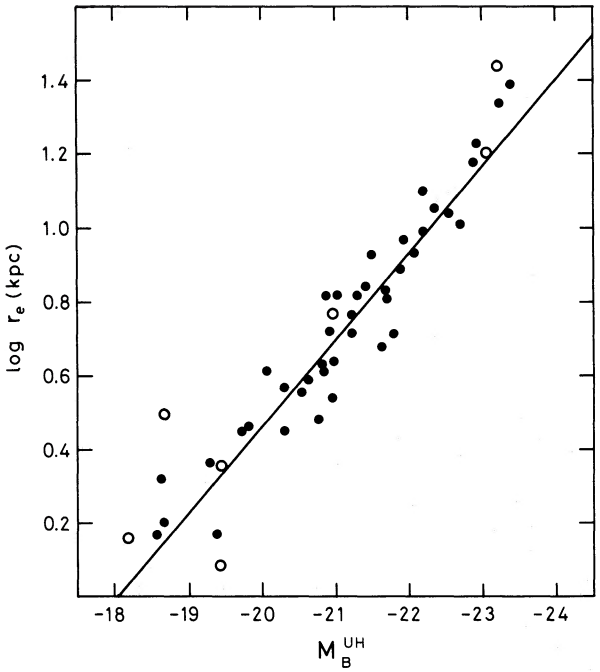

FIG. 8.—Log r_e against absolute magnitude for the ellipticals listed in Table 3. The filled circles show galaxies with r_e determined from the A_e values listed in the RC2. The solid line gives the least-squares power-law fit for these points (eq. [3]). Galaxies with r_e estimated from D_{25} are shown as the open circles.

Together with the dynamical relation $\sigma_0^2 \propto M/r_e$ and the relation between σ_0 and L discussed in § III*d*, equation (3) implies that M/L is approximately independent of L. There is, however, some evidence in our sample for a slight decrease in M/L at low luminosities.

Equation (3) confirms the result found by Tonry and Davis (1981*b*), who studied a larger sample of ellipticals with r_e values taken from the RC2. It is also in good agreement with the relation found by Strom and Strom (1978) from their photometry of galaxies in rich clusters. From a sample of 16 normal ellipticals and 3 lenticular galaxies, Kormendy (1977) derived a different relation. By fitting effective surface brightness to log r_e, he inferred the relation $r_e \propto L^{1.42}$. However, by fitting his values of log r_e to M_B^{UH}, we find $r_e \propto L^{0.8 \pm 0.3}$, which is consistent with equation (3). The difference between the two fits results from the large scatter in the values of r_e over a range of only 2 mag in M_B in the Kormendy (1977) sample. Our relation and the one found by Tonry and Davis (1981*b*) are based mainly on effective radii (half-light radii) derived from standard growth curves, whereas those of Kormendy (1977) and Strom and Strom (1978) are based on $r^{1/4}$-law fits to surface brightness profiles. The details of the fitting procedure and any systematic deviations from the $r^{1/4}$-law with luminosity can bias the relation between r_e and L. In the following discussion, we adopt the relation given by equation (3), but we recognize that it would be desirable to have a homogeneous set of photometry for this sample.

IV. THEORETICAL IMPLICATIONS

a) Hierarchical Clustering Without Dissipation

In the simplest cosmological picture, galaxies, groups, and clusters formed hierarchically by gravitational forces alone. Following Peebles (1974), we assume that the rms density contrast in the primordial distribution of matter had power-law form over a wide range of masses:

$$\langle(\delta\rho/\rho)^2\rangle^{1/2} \propto M^{-1/2-n/6} \; ; \quad -1.5 \lesssim n \lesssim 0 \; . \quad (4)$$

The required value of n is larger for higher values of the cosmological density parameter, the range above being appropriate for $0.1 \lesssim \Omega \lesssim 1$ (Fall 1979*a*). We also assume that the radius-mass relation of the resulting hierarchy may be approximated by a power law:

$$r_i \propto M^{\alpha} \; ; \quad 1/3 < \alpha < (n+5)/6 \; . \quad (5)$$

The value $\alpha = 1/3$ corresponds to all objects forming at the same epoch—the "synchronic" case—and the value $\alpha = (n+5)/6$ corresponds to objects of different masses forming at different epochs—the "diachronic" case (Press and Schechter 1974). The correct relation should lie somewhere between these extremes, but the exact value of α is difficult to predict because it depends on the procedure for identifying individual objects and because substructure may have been destroyed in high-density regions.

A direct consequence of hierarchical clustering is that individual objects would have been set in rotation by the tidal torques of their neighbors. The analytical calculation by Peebles (1969) gives $\lambda_i \approx 0.08$ for the rms spin parameter and no variation with mass in the diachronic case. In general, the value of λ_i and its dependence on M are somewhat uncertain for the same reasons as those given above for the dependence of r_i on M. Thuan and Gott (1977) have suggested a relation of the form $\lambda_i \propto M^{-1/2}$; but their argument depends sensitively on the exclusion of neighboring objects and is not dynamically self-consistent. The N-body simulations of Efstathiou and Jones (1979), in which objects were identified by a synchronic procedure, give $\lambda_i \approx 0.06$ for the median spin parameter and little or no dependence on mass. By fitting to the points in their Figures 4*a* and 4*b*, we find

$$\lambda_i \propto M^{-\beta} \; , \quad \beta = 0.15 \pm 0.15 \; , \quad (6)$$

over a single decade in mass.

As an aid to interpreting the N-body experiments, we have superposed them in Figure 9 on the observed relation between $V_m/\bar{\sigma}$ and absolute magnitude. Scaling for the ordinate was obtained by setting $(V_m/\bar{\sigma})_{\rm model} \approx (\pi/4)(1/0.3)\lambda_{\rm model}$ as appropriate for average orientations. Scaling for the abscissa was based on the determination of 51 mass points as the characteristic mass in the N-body experiments of Efstathiou and Jones (1979) using the method of Schechter and Press (1976) and the conversion $M/L \propto L^{0.16}$. Tammann, Yahil, and Sandage (1979) determine a value $M^*_{B_T} = -20.91$ and a faint end slope of -0.77 for the luminosity function for ellipticals. Correcting this for the sake of consistency to a faint end

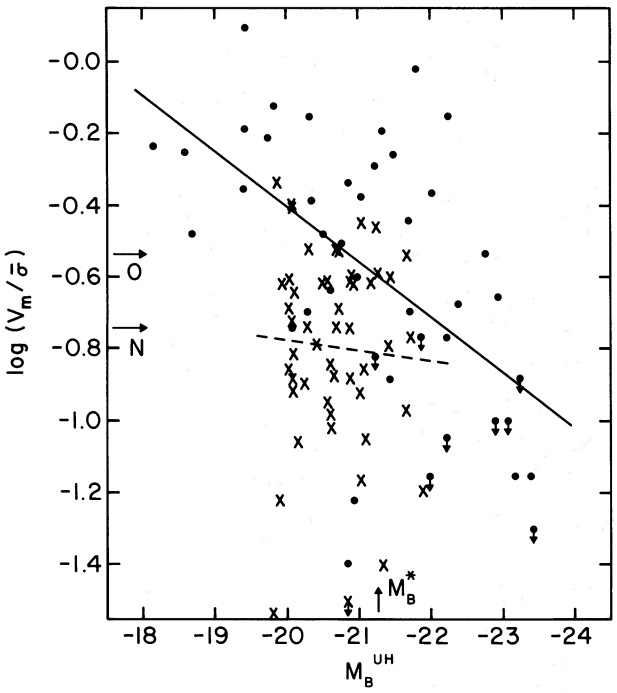

FIG. 9.—Log ($V_m/\bar{\sigma}$) against absolute magnitude, as in Fig. 6. The data (*filled circles*) and fitted relation (*solid line*) are to be compared with the *N*-body points (*crosses*) from Fig. 4*b* of Efstathiou and Jones (1979) and fitted relation (*dashed line*). Scaling of the *N*-body data is described in the text (§ IV*a*). Median values of $V_m/\bar{\sigma}$ for both the observed data (O) and the *N*-body model (N) points are shown, as is M_B^*.

slope of $-5/4$ gives $M_{B_T}^* = -21.26$. We estimate that the uncertainty in this scaling is about 0.5 mag. The amplitude of the observed rotation of faint ellipticals would therefore seem to rule out a nondissipative origin in a clustering hierarchy.

b) Hierarchical Clustering With Dissipation

Some dissipative process is probably necessary to explain the characteristic sizes of galaxies (Rees and Ostriker 1977). We therefore suppose that the "initial" radii and spins of protogalaxies satisfied equations (5) and (6) and that the "final" radii and spins were determined by the amount of energy dissipated during collapse. If the total angular momenta and masses were conserved in the collapse, the following relations must be satisfied:

$$V_m/\bar{\sigma} \propto (r_i/r_e)^{1/2}\lambda_i \,, \tag{7}$$

$$\sigma_0^2 \propto M/r_e \,. \tag{8}$$

With these expressions and the empirical relations of § III, the problem is overconstrained and we can check for consistency.

These relations may be summarized as follows:

$$V_m/\bar{\sigma} \propto L^{-\gamma} \,, \quad \gamma = 0.38 \pm 0.10 \,; \tag{9}$$

$$\sigma_0 \propto L^{\delta} \,, \quad \delta = 0.29 \pm 0.04 \,; \tag{10}$$

$$r_e \propto L^{\epsilon} \,, \quad \epsilon = 0.58 \pm 0.02 \,. \tag{11}$$

Combining equations (6) through (11) gives

$$\alpha - 2\beta = (\epsilon - 2\gamma)/(\epsilon + 2\delta) = -0.16 \pm 0.17 \,, \tag{12}$$

which is lower than predicted by equations (5) and (6) but marginally compatible within the large errors. As Figure 9 shows, the observed values of $V_m/\bar{\sigma}$ at absolute magnitude M_B^* are only twice as large as those provided by nondissipative clustering. To satisfy equation (7), ellipticals must have collapsed by factors of about 4 in the radial direction. The effective radii of these galaxies are, however, at least an order of magnitude smaller than they would be if they joined smoothly onto the hierarchy defined by groups and clusters (Fall 1981). This discrepancy is difficult to reconcile with the idea that ellipticals formed in a clustering hierarchy.

A picture of galaxy formation has been outlined by White and Rees (1978) in which the visible parts of galaxies formed by the dissipative collapse of gas within dark halos. In this case, the final rotation velocity of a galaxy has a nearly linear dependence on the radial collapse factor rather than the square root dependence of equation (7). Fall and Efstathiou (1980) have shown that this picture provides a satisfactory explanation for the origin of disk galaxies. To account for the rapid rotation of the disks in terms of the tidal spin of the halos, the gas must have collapsed by factors of the order of 10. If proto–ellipticals collapsed by this much, they would rotate an order of magnitude faster than observed (see, e.g., Fall 1982).

c) Mergers and Other Possibilities

Toomre (1977) has suggested that ellipticals may have formed by the merging of disk galaxies. This idea has been discussed by several authors within the framework of the White-Rees (1978) picture (Fall 1979*b*; Efstathiou and Jones 1980; Silk and Norman 1981). The rotational properties of merger remnants depend on both the orbital and internal angular momenta of their progenitors. Aarseth and Fall (1980) have shown that the orbital contribution is small, $\lambda_{\rm orb} \approx 0.07$, independent of the masses and sizes of the remnants. In the idealized situation, that N identical disks merge with random orientations from orbits of zero energy, the internal contribution is $\lambda_{\rm int} \approx N^{-3/2}\lambda_{\rm disk}$, where $\lambda_{\rm disk} = 0.43$ is appropriate for the progenitors (Fall 1979*b*). The dependence of λ on the number of merged disks would then be, to rough approximation, the addition of these contributions in quadrature, i.e.,

$$\lambda \approx (\lambda_{\rm orb}^2 + N^{-3}\lambda_{\rm disk}^2)^{1/2} \,. \tag{13}$$

In this picture, $V_m/\bar{\sigma}$ decreases with increasing mass as a result of the statistical cancellation of internal spins, but the exact dependence is difficult to predict in realistic situations. Whether merging can account for the other properties of elliptical galaxies is a topic of current debate (Tremaine 1981).

The rotation properties of spiral bulges and faint ellipticals ($M_B \gtrsim -20.5$) might suggest a common formation scheme. Larson, Tinsley, and Caldwell (1980) argue that the gas in relatively isolated halos continued its

infall until recently, whereas the gas in clustered halos was dispersed before infall was completed. If it is assumed that the gas in the outer parts of each protogalaxy is of high specific angular momentum compared with the central parts, this process might produce mainly elliptical galaxies in clusters and mainly disk galaxies in the field (see also Binney and Silk 1978). We would also expect a resemblance between bulges and ellipticals, including their kinematic properties. A problem with this scheme is that the luminosity functions for bulges and ellipticals are quite different at their bright ends (i.e., there are few disk galaxies with bulges as bright as M87). Moreover, we emphasize that it is not yet clear whether bulges show the same trend between $V_m/\bar{\sigma}$ and luminosity as do the ellipticals.

d) *Pancakes and Blast Waves*

An alternative to hierarchical clustering is the pancake picture of Zeldovich and his colleagues (Sunyaev and Zeldovich 1972; Doroshkevich, Shandarin, and Saar 1978, and references therein). In this case, density perturbations on scales smaller than 10^{14}–10^{15} $M_\odot$ were absent or damped in the primordial distribution of matter, and those on larger scales were subsequently focused by gravity into sheetlike configurations. Material flowing into such pancakes would have acquired some vorticity while crossing the surrounding shocks and would have developed turbulence with subsonic or transonic velocities. (Doroshkevich 1973; Binney 1974). The internal structure of a pancake should consist of a dense layer of cool gas ($T \sim 10^4$ K) compressed between two layers of shock-heated gas ($T \sim 10^6$ K). Subgalactic clouds and protogalaxies are thought to have condensed in cool regions as the result of thermal and gravitational instabilities, and their rotation is thought to be the result of chaotic motions.

For comparison with the empirical relations, we assume an initial radius-mass relation of the form

$$r_i \propto M^\alpha \; ; \quad 1/3 < \alpha < 1/2 \; . \tag{14}$$

This range of α includes the extreme cases in which the major diameters of protogalaxies were much smaller or much larger than the thickness of the pancakes. We also assume that the relation between the initial rotation velocities and sizes may be approximated by a power law:

$$V_{\rm turb} \propto r_i^\mu \; ; \quad 0 < \mu < 1/3 \; . \tag{15}$$

The exponent above should reflect the development and Mach number of the turbulence when protogalaxies began to collapse, with $\mu = 0$ appropriate for the spectrum just behind the shocks and $\mu = 1/3$ for a Kolmogorov spectrum. Doroshkevich, Shandarin, and Saar (1978) advocate the values $\alpha = 3/7$ and $\mu = 0$. We can now check for consistency by arguments similar to those used in § III*b*; in this case, conservation of angular momentum and mass implies

$$(1 + \mu)\alpha = (\epsilon + \delta - \gamma)/(2\delta + \epsilon) = 0.42 \pm 0.09 \; , \tag{16}$$

which agrees remarkably well with the predictions.

This picture makes two additional predictions about the rotation of galaxies (Doroshkevich 1973). (*a*) Galaxies that formed near the centers of the pancakes should have lower specific angular momenta than those that formed in the outer parts. (*b*) The rotation axes of galaxies should show some tendency to lie in the plane of the pancake in which they formed. To the extent that the morphology of galaxies is a rough indicator of their specific angular momenta, the clustering properties of spheroidal and disk galaxies are in qualitative agreement with the first prediction (Hubble and Humanson 1931; Dressler 1980*a*). Several attempts have been made to test the second prediction, with the result that there is no compelling evidence for alignments between the minor axes of galaxies and the major axes of clusters or superclusters (Hawley and Peebles 1975; MacGillivray *et al.* 1982, and references therein). Whether this is a serious problem for the pancake picture or whether it is due to idealizations in the original formulation remains to be seen.

Ostriker and Cowie (1981) and Ikeuchi (1981) have recently suggested that the formation of galaxies was triggered by blast waves from explosions in other galaxies or quasars. The first generation of structure, which provided the seeds for this process, may have been developed either hierarchically or in pancakes. The majority of galaxies would have condensed later from cool and turbulent gas that was swept up by the blast waves. Although these sheets are expected to have been rather different from the pancakes of the previous picture, the physical processes and geometrical configurations may have been similar. If so, the arguments that led to equation (16) should apply to this picture as well. Moreover, since each blast wave is expected to have produced a small group rather than a large cluster of galaxies, the lack of alignment in their rotation axes is unlikely to be a problem. Whether the picture with blast waves can account for the other properties of galaxies, including those of different morphological types, is not yet clear.

NOTE.—The parameter r is in arc seconds, while V and σ are given in km s^{-1}. Heliocentric velocities for six additional galaxies (listed in Table 2A) measured at the AAT for central dispersions are 1228 km s^{-1} (NGC 3608), 1757 km s^{-1} (NGC 3136), 1800 km s^{-1} (NGC 3923), 1776 km s^{-1} (NGC 3962), 658 km s^{-1} (NGC 4458), and 958 km s^{-1} (NGC 4489).

[a] Heliocentric systemic velocities derived from the HGVS data. Mean values from cross-correlation against four different standard stars.

[b] Heliocentric systemic velocities from the IPCS data, based on the Tonry and Davis 1981*a* velocities, have been corrected as described in the Appendix.

TABLE 5

ROTATION VELOCITY AND VELOCITY DISPERSION DATA

r	V	ΔV	σ	Δσ	γ	Δγ
		NGC 2778	v^a = 2035 km s^{-1}			
23.3	-96	39	130	68	0.70	0.15
13.8	-137	23	96	49	0.63	0.08
10.4	-109	22	131	37	0.73	0.09
7.6	-102	15	105	30	0.71	0.06
4.7	-79	11	132	19	0.88	0.06
2.8	-36	8	137	13	0.94	0.04
1.4	-14	7	156	11	1.01	0.04
0.0	3	10	178	14	1.04	0.05
-1.4	5	12	200	17	1.00	0.06
-2.8	38	13	158	20	0.93	0.06
-4.2	75	13	101	26	0.77	0.06
-6.2	84	14	110	27	0.72	0.06
-9.0	99	20	136	34	0.79	0.09
-11.8	96	27	153	42	0.75	0.11
-15.2	61	24	132	41	0.89	0.12
-21.0	89	28	195	43	0.95	0.13
		NGC 3605	v^a = 673 km s^{-1}			
20.7	81	13	115	22	0.90	0.11
13.8	65	11	84	17	0.84	0.09
10.4	50	8	69	14	0.82	0.07
7.6	36	7	86	11	1.05	0.07
4.8	25	5	100	7	1.12	0.05
2.8	10	5	95	8	1.12	0.05
1.4	-1	4	87	6	1.11	0.04
0.0	-7	4	87	6	1.14	0.04
-1.4	-12	4	100	6	1.20	0.05
-2.8	-24	5	97	7	1.16	0.05
-4.2	-32	5	85	8	1.07	0.05
-6.2	-39	6	91	9	1.05	0.06
-9.0	-46	8	71	12	0.87	0.06
-11.8	-48	11	99	17	0.95	0.09
-15.1	-55	13	116	19	1.17	0.13
-19.9	-35	16	80	27	0.78	0.12
		NGC 3818	v^b = 1700 km s^{-1}			
15.3	93	15	91	21	0.61	0.06
9.7	125	11	120	12	0.74	0.05
6.4	108	12	132	12	0.72	0.05
4.0	86	12	145	11	0.71	0.05
1.7	58	13	159	12	0.77	0.06
-0.7	-6	8	196	7	1.00	0.05
-3.1	-65	10	177	9	0.83	0.05
-5.4	-105	13	129	13	0.66	0.05
-7.8	-116	14	121	17	0.69	0.06
-11.1	-102	14	115	16	0.71	0.06
-16.7	-79	17	140	17	0.64	0.07
		NGC 3904	v^b = 1682 km s^{-1}			
25.6	67	26	167	23	0.63	0.11
17.5	67	16	199	14	0.75	0.08
11.8	51	14	172	12	0.76	0.07
8.4	19	14	205	11	0.84	0.07
6.1	20	14	211	12	0.82	0.07
3.7	34	14	234	10	0.75	0.06
1.4	28	11	198	8	0.94	0.06
-1.0	-33	12	196	9	0.90	0.07
-3.4	-49	16	188	14	0.72	0.07
-5.7	-21	13	185	12	0.78	0.06
-8.1	-39	17	206	13	0.80	0.09
-11.4	-26	14	193	12	0.90	0.08
-17.1	-56	16	177	14	0.75	0.08
-25.2	-61	25	148	22	0.54	0.09
		NGC 4387	v^a = 575 km s^{-1}			
23.3	86	33	95	50	0.54	0.16
17.9	41	13	47	25	0.84	0.11
13.8	42	9	69	15	0.94	0.08
10.4	45	10	100	15	0.99	0.09
7.6	51	8	101	11	1.00	0.07
4.8	35	5	100	8	1.03	0.05
2.8	30	6	97	8	1.02	0.05
1.4	17	5	103	7	1.09	0.05
0.0	1	5	111	7	1.19	0.05
-1.4	-4	5	116	7	1.22	0.05
-2.8	-11	5	111	7	1.20	0.06
-4.2	-16	5	98	8	1.14	0.05
-6.2	-27	6	96	9	1.08	0.06
-9.0	-51	9	92	13	1.02	0.08
-11.8	-54	12	110	17	0.96	0.10
-15.1	-70	13	82	20	0.77	0.09
-19.3	-58	23	81	36	0.63	0.13
-24.6	-72	23	58	42	0.64	0.15

r	V	ΔV	σ	Δσ	γ	Δγ
		NGC 4478	v^b = 1365 km s^{-1}			
25.7	-68	18	110	22	0.69	0.08
17.8	-58	13	99	16	0.75	0.06
12.2	-66	12	121	13	0.75	0.06
8.8	-50	12	128	13	0.77	0.05
6.5	-45	10	132	11	0.79	0.05
4.1	-35	11	145	10	0.84	0.05
1.8	-24	12	148	11	0.92	0.07
-0.6	9	8	145	7	0.94	0.04
-3.0	22	8	148	8	0.88	0.04
-5.3	36	8	140	8	0.81	0.05
-7.7	48	9	135	9	0.80	0.05
-10.0	46	10	145	10	0.81	0.05
-13.4	55	9	124	9	0.81	0.04
-19.0	49	11	94	15	0.75	0.05
-26.9	77	19	79	32	0.59	0.07
		NGC 4551	v^a = 1217 km s^{-1}			
25.1	70	19	75	32	0.73	0.14
18.0	47	15	69	25	0.84	0.13
13.8	27	12	91	19	0.96	0.11
10.4	46	11	111	16	1.01	0.10
7.6	43	9	99	13	1.00	0.08
4.8	26	8	121	11	1.19	0.08
2.8	8	7	114	10	1.21	0.07
1.4	3	7	108	10	1.13	0.07
0.0	-10	6	109	9	1.11	0.06
-1.4	-23	6	115	8	1.15	0.06
-2.8	-28	6	115	9	1.22	0.07
-4.2	-32	7	106	10	1.12	0.07
-6.2	-34	8	120	12	1.09	0.08
-9.0	-21	12	135	17	1.10	0.11
-11.8	-34	12	80	20	0.83	0.10
-15.2	-21	13	115	18	1.13	0.13
-19.3	-40	28	63	47	0.44	0.12
-30.7	-30	18	91	30	0.96	0.16
		NGC 4742	v^b = 1297 km s^{-1}			
17.5	80	12	29	47	0.52	0.04
11.8	81	11	49	44	0.57	0.04
8.5	81	10	54	21	0.57	0.04
6.1	76	8	64	15	0.58	0.03
3.7	78	11	52	24	0.47	0.03
1.4	36	11	85	16	0.56	0.04
-1.0	-26	11	110	14	0.83	0.06
-3.3	-102	13	67	18	0.61	0.05
-5.7	-90	13	55	19	0.54	0.05
-8.1	-80	11	64	22	0.61	0.04
-10.4	-87	11	66	17	0.64	0.04
-13.8	-84	12	67	21	0.62	0.05
-19.5	-74	14	61	28	0.63	0.06
		NGC 5638	v^b = 1637 km s^{-1}			
14.5	-69	14	124	15	0.87	0.08
8.0	-43	12	136	12	0.77	0.07
4.6	-38	13	148	13	0.85	0.07
2.4	-36	12	158	11	0.86	0.07
0.0	0	9	154	8	0.96	0.05
-2.4	22	12	161	11	0.96	0.07
-4.6	28	13	152	12	0.83	0.07
-8.0	40	12	157	11	0.87	0.06
-14.6	95	13	111	15	0.75	0.06
		NGC 5831	v^b = 1636 km s^{-1}			
15.2	17	17	149	17	0.73	0.08
8.7	7	12	133	13	0.78	0.06
5.4	-28	14	144	14	0.80	0.07
3.1	-20	15	155	15	0.75	0.07
0.7	-6	10	152	9	0.97	0.06
-1.7	14	11	156	10	0.99	0.07
-4.0	27	13	174	11	0.79	0.06
-6.4	-10	12	144	12	0.74	0.06
-9.7	2	12	125	13	0.70	0.05
-16.2	-3	16	150	14	0.69	0.07
		NGC 5845	v^b = 1439 km s^{-1}			
16.4	151	28	103	36	0.53	0.10
9.6	146	12	120	14	0.79	0.06
6.4	130	12	123	12	0.75	0.05
4.0	132	12	173	11	0.78	0.06
1.7	107	12	210	9	0.83	0.06
-0.7	-37	11	263	8	1.09	0.08
-3.1	-115	11	180	9	0.78	0.05
-5.4	-114	13	145	12	0.76	0.06
-7.8	-135	14	129	15	0.74	0.06
-11.0	-130	15	90	19	0.66	0.06
-17.9	-109	30	51	56	0.38	0.08

V. CONCLUSIONS

We have obtained major axis spectra of 17 elliptical galaxies at the 4 m telescopes of the AAO and KPNO. These galaxies have absolute magnitudes comparable to the bulges of disk galaxies and are fainter than most of the ellipticals studied to date. For 11 of the galaxies, our data are of high enough quality that we have been able to derive accurate rotation curves and dispersion profiles out to the effective radius of each galaxy.

To search for trends in the kinematic properties of galaxies, we have combined our measurements with those from previous studies. The result is a compilation that includes 50 ellipticals over a range of two decades in luminosity and 8 bulges over a smaller range in luminosity. We have found that, for the ellipticals, $V_m/\bar{\sigma}$ is a decreasing function of luminosity. The scatter at the bright end of this relation is larger than would be expected from the observational errors alone. There appear to be no selection effects that would bias this relation, and in particular, there is no correlation of ellipticity with absolute magnitude. The faint ellipticals and bulges rotate nearly as rapidly as predicted by models with oblate figures and isotropic distributions of residual velocities. From the limited sample of bulges, it is not possible to determine the dependence of $V_m/\bar{\sigma}$ on luminosity. The relation between the central velocity dispersion and luminosity of the ellipticals is consistent with previous determinations; however, we find some evidence for a slightly stronger dependence than $\sigma_0 \propto L^{1/4}$ and some evidence for curvature at the faint end.

We have compared these results with the predictions of several theories for the formation of galaxies. The observed decrease of $V_m/\bar{\sigma}$ with mass may be compatible with the formation of elliptical galaxies in a clustering hierarchy, but the low values of $V_m/\bar{\sigma}$ for bright ellipticals are difficult to reconcile with their high densities. The dependence of $V_m/\bar{\sigma}$ on mass is in the sense expected if ellipticals formed by merging or by fragmentation in pancakes or blast waves.

We thank S. M. Faber for helpful comments on an earlier version of this paper. R. L. D. is grateful to Christ's College, Cambridge, for providing financial support. S. M. F. and G. I. thank the director and staff of the Institut d'Astrophysique, Paris, for hospitality during the CECAM workshop in 1981 August. R. L. D. and G. I. are grateful for the support of NATO research grant RG 179.81 during the latter part of this project. G. I. appreciates the hospitality of the Institute of Astronomy, Cambridge, during the course of this project. The authors are grateful for the use of the Cambridge Starlink node for data analysis.

APPENDIX

Rotation velocity, V, velocity dispersion, σ, and line strength, γ, along the major axis are tabulated in Table 5 for the 11 galaxies with long integrations. Errors ΔV, $\Delta\sigma$, and $\Delta\gamma$ are also given. All velocities are in km s^{-1}, and all radii, are in arc seconds, with negative radii for data *east* of the N-S line. Heliocentric systemic velocities for the HGVS data (see note *a*) are mean values derived from the cross-correlation against the standard stars in Table 2B. The internal uncertainty in these velocities is $\lesssim$20 km s^{-1}. The systemic velocities for the IPCS data (see note *b*) have been tied to the velocity scale of Tonry and Davis (1981*a*) and have been corrected for the zero-point difference, $\langle V_{\rm IPCS} - V_{\rm TD}\rangle = 17$ km s^{-1}. After correction the rms scatter is $\langle (V_{\rm IPCS} - V_{\rm TD})^2\rangle^{1/2} = 26$ km s^{-1}.

REFERENCES

Aarseth, S. J., and Fall, S. M. 1980, *Ap. J.*, **236**, 43.
Bertola, F., and Capaccioli, M. 1975, *Ap. J.*, **200**, 439.
Binney, J. 1974, *M.N.R.A.S.*, **168**, 73.
———. 1978, *M.N.R.A.S.*, **183**, 501.
———. 1980, *M.N.R.A.S.*, **190**, 421.
———. 1981, in *The Structure and Evolution of Normal Galaxies*, ed. S. M. Fall and D. Lynden-Bell (Cambridge: Cambridge University Press), p. 55.
Binney, J., and Silk, J. 1978, *Comm. Astr. Ap.*, **7**, 139.
Carter, D., Efstathiou, G., Ellis, R. S., Inglis, I., and Godwin, J. 1981, *M.N.R.A.S.*, **195**, 15P.
Davies, R. L. 1979, Ph. D. thesis, University of Cambridge.
———. 1981, *M.N.R.A.S.*, **194**, 879.
Davies, R. L., and Illingworth, G. 1983, *Ap. J.*, **266**, in press.
de Vaucouleurs, G. 1959, *Handbuch der Physik*, **53**, 311.
———. 1975, in *Stars and Stellar Systems*, Vol. **9**, *Galaxies and the Universe*, ed. A. Sandage, M. Sandage, and J. Kristian (Chicago: University of Chicago Press), p. 557.
de Vaucouleurs, G., de Vaucouleurs, A., and Corwin, H. R. 1976, *Second Reference Catalogue of Bright Galaxies*, (Austin: University of Texas Press) (RC2).
de Vaucouleurs, G., and Pence, W. 1979, *Ap. J. Suppl.*, **39**, 49.
Doroshkevich, A. G. 1973, *Soviet Astr.–AJ*, **16**, 986.
Doroshkevich, A. G., Shandarin, S. F., and Saar, E. 1978, *M.N.R.A.S.*, **184**, 643.
Dressler, A. 1978, *Ap. J.*, **226**, 55.
———. 1979, *Ap. J.*, **231**, 659.
———. 1980*a*, *Ap. J.*, **236**, 351.
———. 1980*b*, *Ap. J.* (*Letters*), **240**, L11.
Efstathiou, G., Ellis, R. S., and Carter, D. 1980, *M.N.R.A.S.*, **193**, 931.
———. 1982, *M.N.R.A.S.*, in press.
Efstathiou, G., and Jones, B. J. T. 1979, *M.N.R.A.S.*, **186**, 133.
———. 1980, *Comm. Astr. Ap.*, **8**, 169.
Faber, S. M. 1977, in *The Evolution of Galaxies and Stellar Populations*, ed. B. M. Tinsley and R. B. Larson (New Haven: Yale University Observatory), p. 157.
Faber, S. M., and Jackson, R. E. 1976, *Ap. J.*, **204**, 668.
Fall, S. M. 1979*a*, *Rev. Mod. Phys.*, **51**, 21.
———. 1979*b*, *Nature*, **281**, 200.
———. 1981, in *The Structure and Evolution of Normal Galaxies*, ed. S. M. Fall and D. Lynden-Bell (Cambridge: Cambridge University Press), p. 1.

Fall, S. M., and Efstathiou, G. 1980, *M.N.R.A.S.*, **193**, 189.
Fish, R. A. 1964, *Ap. J.*, **139**, 284.
Hawley, D. L., and Peebles, P. J. E. 1975, *A.J.*, **80**, 477.
Hubble, E., and Humanson, M. L. 1931, *Ap. J.*, **74**, 43.
Ikeuchi 1981, *Pub. Astr. Soc. Japan*, **33**, 211.
Illingworth, G. 1977, *Ap. J. (Letters)*, **218**, L43.
———. 1981, in *The Structure and Evolution of Normal Galaxies*, ed. S. M. Fall and D. Lynden-Bell (Cambridge: Cambridge University Press), p. 27.
Illingworth, G., and Schechter, P. L. 1982, *Ap. J.*, **256**, 481.
King, I. R. 1978, *Ap. J.*, **222**, 1.
Kormendy, J. 1977, *Ap. J.*, **218**, 333.
———. 1982, *Ap. J.*, **257**, 75.
Kormendy, J., and Illingworth, G. 1982, *Ap. J.*, **256**, 460.
Larson, R. B. 1975, *M.N.R.A.S.*, **173**, 671.
Larson, R. B., Tinsley, B. M., and Caldwell, C. N. 1980, *Ap. J.*, **237**, 692.
Lauberts, A., Holmberg, E. B., Schuster, H. E., and West, R. M. 1981, *Astr. Ap. Suppl.*, **46**, 311.
Leach, R. W. 1981, *Ap. J.*, **248**, 485.
MacGillivray, H. T., Dodd, R. J., McNally, B. V., and Corwin, H. G. 1982, *M.N.R.A.S.*, **198**, 605.
Malamuth, E., and Kirshner, R. P. 1981, *Ap. J.*, **251**, 508.
Mould, J., Aaronson, M., and Huchra, J. 1980, *Ap. J.*, **238**, 458.
Nilson, P. N. 1973, *Uppsala General Catalogue of Galaxies* (*Uppsala Astr. Obs. Ann.*, Vol. **6**) (UGC).
Ostriker, J. P., and Cowie, L. L. 1981, *Ap. J. (Letters)*, **243**, L127.
Peebles, P. J. E. 1969, *Ap. J.*, **155**, 393.
———. 1974, *Ap. J. (Letters)*, **189**, L51.
Peterson, C. J. 1978, *Ap. J.*, **222**, 84.
Press, W. H., and Schechter, P. L. 1974, *Ap. J.*, **187**, 425.
Rees, M. J., and Ostriker, J. P. 1977, *M.N.R.A.S.*, **179**, 541.
Rood, H. 1981, unpublished compilation of redshifts.
Sandage, A. 1973, *Ap. J.*, **183**, 711.
———. 1978, *A.J.*, **83**, 904.
Sandage, A., Freeman, K. C., and Stokes, N. R. 1970, *Ap. J.*, **160**, 831.
Sandage, A., and Visvanathan, N. 1978, *Ap. J.*, **225**, 742.
Sandage, A., and Tammann, G. A. 1981, *A Revised Shapley-Ames Catalog of Bright Galaxies*, (Washington, D.C.: Carnegie Institution of Washington), Publication 635 (RSA).
Sargent, W. L. W., Schechter, P. L., Boksenberg, A., and Shortridge, K. 1977, *Ap. J.*, **212**, 326.
Sargent, W. L. W., Young, P. J., Boksenberg, A., Shortridge, K., Lynds, C. R., and Hartwick, F. D. A. 1978, *Ap. J.*, **221**, 731.
Schechter, P. L. 1980, *A.J.*, **85**, 801.
Schechter, P. L., and Gunn, J. E. 1979, *Ap. J.*, **229**, 472.
Schechter, P. L., and Press, W. H. 1976, *Ap. J.*, **203**, 557.
Silk, J., and Norman, C. 1981, *Ap. J.*, **247**, 59.
Strom, S. E., and Strom, K. M. 1978, *Ap. J. (Letters)*, **225**, L93.
Sunyaev, R. A., and Zeldovich, Y. B. 1972, *Astr. Ap.*, **20**, 189.
Tammann, G. A., Yahil, A., and Sandage, A. 1979, *Ap. J.*, **234**, 775.
Terlevich, R., Davies, R. L., Faber, S. M., and Burstein, D. 1981, *M.N.R.A.S.*, **196**, 381.
Thuan, T. X., and Gott, J. R. 1977, *Ap. J.*, **216**, 194.
Tonry, J. L. 1981, *Ap. J. (Letters)*, **251**, L1.
Tonry, J. L., and Davis, M. 1980, *A.J.*, **84**, 1511.
———. 1981*a*, *Ap. J.*, **246**, 666.
———. 1981*b*, *Ap. J.*, **246**, 680.
Toomre, A. 1977, in *The Evolution of Galaxies and Stellar Populations*, ed. B. M. Tinsley and R. B. Larson (New Haven: Yale University Observatory), p. 401.
Tremaine, S. 1981, in *The Structure and Evolution of Normal Galaxies*, ed. S. M. Fall and D. Lynden-Bell (Cambridge: Cambridge University Press), p. 67.
White, S. D. M. 1979, *M.N.R.A.S.*, **189**, 831.
White, S. D. M., and Rees, M. J. 1978, *M.N.R.A.S.*, **183**, 341.
Whitmore, B. C., Kirshner, R. P., and Schechter, P. L. 1979, *Ap. J.*, **234**, 68.
Williams, T. B. 1979, in *Photometry, Kinematics, and Dynamics of Galaxies*, ed. D. Evans, (Austin: University of Texas Press), p. 187.
Young, P. J., Sargent, W. L. W., Boksenberg, A., Lynds, C. R., and Hartwick, F. D. A. 1978, *Ap. J.*, **222**, 450.
Zwicky, F., Herzog, E., Wild, P., Karpowicz, M., and Kowal, C. T. 1961–1968, *Catalogue of Galaxies and Clusters of Galaxies*, 6 Vols. (Pasadena: California Institute of Technology).

ROGER L. DAVIES, GARTH ILLINGWORTH and PAUL L. SCHECHTER: Kitt Peak National Observatory, P.O. Box 26732, Tucson, AZ 85726

GEORGE EFSTATHIOU and S. MICHAEL FALL: Institute of Astronomy, Madingley Road, Cambridge CB3 0HA, England, UK